Molecular Plant
Research Article

CellPress
PARTNER JOURNAL

SUMOylation Inhibition Mediated by Disruption of SUMO E1-E2 Interactions Confers Plant Susceptibility to Necrotrophic Fungal Pathogens

Laura Castaño-Miquel, Abraham Mas, Inês Teixeira, Josep Seguí, Anna Perearnau, Bhagyasree N. Thampi, Arnaldo L. Schapire, Natalia Rodrigo, Gaelle La Verde, Silvia Manrique, Maria Coca and L. Maria Lois*

Center for Research in Agricultural Genomics – CRAG, Edifici CRAG-Campus UAB, Bellaterra (Cerdanyola del Vallés), 08193 Barcelona, Spain

*Correspondence: L. Maria Lois (maria.lois@cragenomica.es)

http://dx.doi.org/10.1016/j.molp.2017.01.007

ABSTRACT

Protein modification by SUMO modulates essential biological processes in eukaryotes. SUMOylation is facilitated by sequential action of the E1-activating, E2-conjugating, and E3-ligase enzymes. In plants, SUMO regulates plant development and stress responses, which are key determinants in agricultural productivity. To generate additional tools for advancing our knowledge about the SUMO biology, we have developed a strategy for inhibiting *in vivo* SUMO conjugation based on disruption of SUMO E1-E2 interactions through expression of E1 SAE2^{UFDCt} domain. Targeted mutagenesis and phylogenetic analyses revealed that this inhibition involves a short motif in SAE2^{UFDCt} highly divergent across kingdoms. Transgenic plants expressing the SAE2^{UFDCt} domain displayed dose-dependent inhibition of SUMO conjugation, and have revealed the existence of a post-transcriptional mechanism that regulates SUMO E2 conjugating enzyme levels. Interestingly, these transgenic plants displayed increased susceptibility to necrotrophic fungal infections by *Botrytis cinerea* and *Plectosphaerella cucumerina*. Early after fungal inoculation, host SUMO conjugation was post-transcriptionally downregulated, suggesting that targeting SUMOylation machinery could constitute a novel mechanism for fungal pathogenicity. These findings support the role of SUMOylation as a mechanism involved in plant protection from environmental stresses. In addition, the strategy for inhibiting SUMO conjugation *in vivo* described in this study might be applicable in important crop plants and other non-plant organisms regardless of their genetic complexity.

Key words: SUMO inhibition, development, flowering, necrotrophic fungi, E1-activating enzyme, E1–E2 interaction disruption

Castaño-Miquel L., Mas A., Teixeira I., Seguí J., Perearnau A., Thampi B.N., Schapire A.L., Rodrigo N., La Verde G., Manrique S., Coca M., and Lois L.M. (2017). SUMOylation Inhibition Mediated by Disruption of SUMO E1-E2 Interactions Confers Plant Susceptibility to Necrotrophic Fungal Pathogens. Mol. Plant. **10**, 709–720.

INTRODUCTION

In response to external and internal cues, plants develop finely tuned growth programs adapted to environmental conditions and developmental stage (Naseem et al., 2015). Protein post-translational regulation by small ubiquitin-like modifier (SUMO) conjugation has emerged as a major molecular mechanism regulating plant growth and stress responses. As ubiquitin, SUMO is attached to protein targets through sequential reactions catalyzed by the E1, E2, and E3 enzymes (Gareau and Lima, 2010). SUMO proteases are responsible for SUMO maturation and deconjugation (Gareau and Lima, 2010).

SUMO activation is a two-step ATP-dependent reaction catalyzed by the heterodimeric E1-activating enzyme, SAE2/SAE1, which is the first control point to enter the conjugation cascade (Supplemental Figure 1) (Walden et al., 2003; Castaño-Miquel et al., 2011). SAE2 is structured in four functional domains: adenylation, catalytic cysteine (SAE2^{Cys}), ubiquitin-fold (domain structurally resembling ubiquitin, SAE2^{UFD}), and C-terminal (SAE2^{Ct}) domains (Lois and Lima, 2005). The E1 activating

Published by the Molecular Plant Shanghai Editorial Office in association with Cell Press, an imprint of Elsevier Inc., on behalf of CSPB and IPPE, SIBS, CAS.

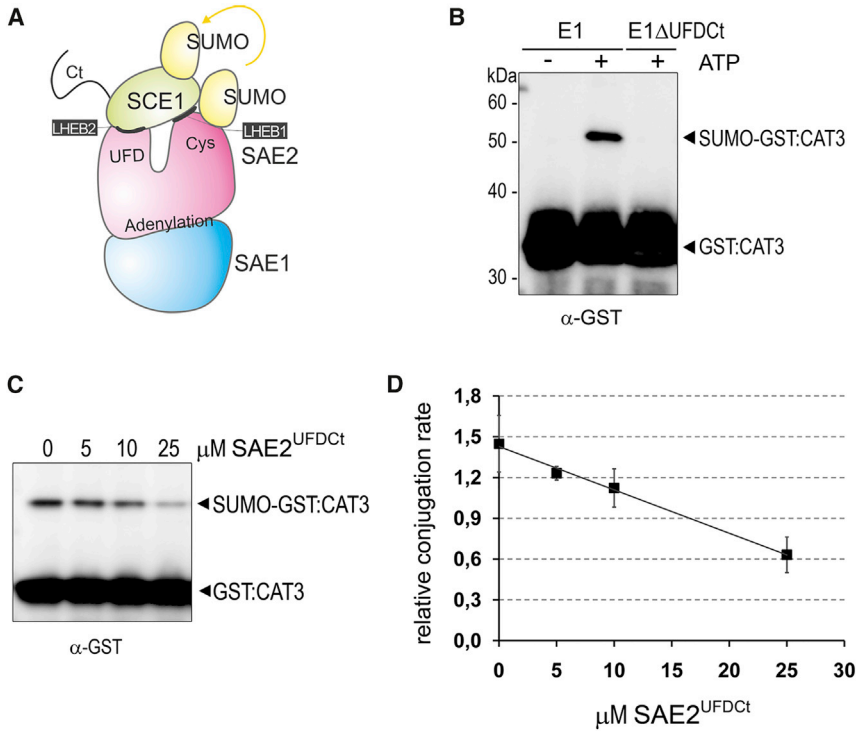

Figure 1. Engineering SUMO Activating Enzyme Large Subunit, SAE2, for SUMOylation Inhibition by Blocking E1 (SAE2/SAE1) and E2 (SCE1) Interactions.

(A) Schematic representation of protein-protein interactions during SUMO transfer from the E1 to the E2.

(B) SAE2^{UFDCt} domain (Ser436-Glu625) is essential for SUMO conjugation *in vitro*. SUMOylation assays were performed in the presence of *Arabidopsis* E1 (SAE2/SAE1a) or the deletion mutant E1ΔUFDCt (SAE2 ΔUFDCt/SAE1a), SUMO2, SCE1, and GST:CAT3Ct as substrate. Reactions in the absence of ATP were performed as negative control. Reaction mixtures were incubated at 37°C and stopped after 15 min of incubation. Reaction products were resolved by SDS-PAGE and examined by immunoblot analysis with anti-GST antibodies.

(C and D) SAE2^{UFDCt} inhibits SUMO conjugation *in vitro*. **(C)** SUMOylation assays were performed at 37°C in the presence of E1, SUMO2, SCE1, and GST:CAT3Ct as a substrate, and in the absence or increasing amounts of SAE2^{UFDCt}. Reaction mixtures were stopped after 30 min and products were analyzed as in **(B)**. Reactions were performed in quadruplicates and relative GST:CAT3Ct sumoylation quantified. Average values and SEM bars are plotted on the graph **(D)**.

enzyme small subunit, SAE1, contributes the essential Arg21 to the adenylation domain (Lee and Schindelin, 2008). The adenylation domain is responsible for SUMO recognition and SUMO C-terminal adenylation. After adenylation, the SUMO C-terminal adenylate establishes a thioester bond with the E1 catalytic cysteine. Following thioester bond formation, SUMO can be transferred to the E2-conjugating enzyme in a reaction that involves E2 recruitment through the two interacting surfaces (Lois and Lima, 2005; Wang et al., 2007, 2010; Reiter et al., 2015) (Figure 1A). On one hand, the SAE2^{UFD} domain establishes contacts with residues located at the α1-helix and the β1β2-loop of the E2 conjugating enzyme (Wang et al., 2009, 2010; Reiter et al., 2015). On the other, the SAE2^{Cys} domain interacts with residues located at the E2 α4 N-terminus (Wang et al., 2007). Although both interactions surfaces involved SAE2 residues present in loops, SAE2^{UFD}-E2 interactions display higher affinity (K_D = 1.2 μM) (Reiter et al., 2013) than SAE2^{Cys}-E2 interactions (K_D = 80 μM) (Wang et al., 2007), supporting a major role of the SAE2^{UFD} domain in E2 recruitment. Even though the SAE2^{UFD} domain is essential in yeast (Lois and Lima, 2005), it remains unclear whether SAE2^{UFD} is sufficient for efficient E2 recruitment *in vivo*.

In plants, SUMOylation has been shown to modulate plant hormone signaling (Lois et al., 2003; Miura et al., 2009; Conti et al., 2014), root stem cell maintenance (Xu et al., 2013), and responses to abiotic and biotic stress (Lois, 2010). Many of the plant biological processes regulated by SUMOylation have been uncovered by the analysis of proteases and SUMO E3 ligase mutant plants, which display pleiotropic growth defects and reduced viability (Murtas et al., 2003; Miura et al., 2005; Huang et al., 2009; Ishida et al., 2009). Nonetheless, some of these mutations have also been proposed to confer adaptive responses to some stresses, such as salt, drought, resistance to plant viruses, and salicylic acid-mediated plant immunity (Yoo et al., 2006; Lee et al., 2007; Miura et al., 2011, 2013; Saleh et al., 2015).

Despite the important agronomic traits regulated by SUMO, most research studies on SUMOylation have been mainly limited to model plants, such as *Arabidopsis* and rice (Wang et al., 2011), due to the lack of molecular tools specific to other economically relevant plants. On the other hand, plants harboring mutations in main components of the SUMOylation machinery, such as *Arabidopsis siz1* (Miura et al., 2010), *mms21* (Huang et al., 2009; Ishida et al., 2009), or *esd4* (Murtas et al., 2003), display severe growth defects that are dependent on salicylic acid accumulation (Miura et al., 2010; Villajuana-Bonequi et al., 2014). The development of tools alternative to null mutants are of great interest in overcoming these technical constraints.

Considering the relevance of SUMO as a major post-translational modification, it is expected that novel biological functions regulated by SUMO remain to be uncovered. Necrotrophic pathogens, such as *Botrytis cinerea* and *Plectosphaerella cucumerina*, promote host cell death to acquire nutrients for proliferation on dead and decaying tissues. Defense responses regulated by the salicylic acid-dependent pathway and associated to programmed cell death are effective against biotrophic pathogens; however, they benefit necrotrophic pathogens. Control of necrotrophic infections is achieved by a different set of defense responses activated by jasmonic acid and ethylene signaling (Glazebrook, 2005). Despite recent progress, how plants perceive and respond to necrotrophy is behind our understanding of plant responses to biotrophy (Mengiste, 2012).

Here, we have developed an innovative strategy for inhibiting SUMO conjugation *in vivo* as an alternative to knock-out mutants, which are lethal, in the case of E1-activating and E2-conjugating enzymes, or display strong pleiotropic phenotypes, in the case of E3 ligases. We have shown that SAE2^{UFDCt} functions as a SUMO conjugation inhibitor both *in vitro* and *in vivo* in a dose-dependent manner, through a mechanism based on its ability to establish non-covalent interactions with the SUMO E2-conjugating enzyme. Our results showed that the SAE2^{UFDCt} domain is sufficient for E2 recruitment *in vivo*, providing a novel molecular target for developing small molecule SUMO conjugation inhibitors. SAE2^{UFDCt} expression is robust and stable through plant generations, and has allowed a novel post-transcriptional regulation of *in vivo* SUMO E2-conjugating enzyme levels to be uncovered. In addition, the study of these plants has facilitated the identification of a novel role of SUMO in defense responses against necrotrophic fungal pathogens. The use of SAE2^{UFDCt} expressing lines have provided an advantage over the use of *siz1* E3 ligase knock-out mutants by allowing the analysis of plant susceptibility to fungal pathogens under different degrees of SUMOylation inhibition. Our results indicate that SUMOylation is required for resistance to necrotrophic fungal attacks. During infection, free and conjugated SUMO, the E1-activating enzyme large subunit SAE2, and the E2-conjugating enzyme SCE1 diminished. In summary, we provide a novel strategy for SUMOylation inhibition that is easy to implement in any transformable plant regardless of its genetic complexity, which has been validated by uncovering a novel regulatory role of SUMO in defense responses to necrotrophic fungi. Our findings suggest that depleting host SUMO conjugation machinery could constitute a novel mechanism for fungal pathogenicity.

RESULTS

SAE2^{UFDCt} Is Essential for *Arabidopsis* SUMO E1 Activity and, as Independent Domain, Inhibits SUMO Conjugation

To develop an innovative strategy for inhibiting SUMOylation that could be easily implemented in any transformable organism of interest, plant, or animal, we have exploited the disruption of SUMO E1-activating and E2-conjugating enzyme interactions (Figure 1A). Previous studies identified two independent regions in the SUMO E1 large subunit SAE2 involved in E2 interactions located at the SAE2 Cys domain and ubiquitin-fold domain (UFD), respectively. We performed comparative analyses of SAE2 protein orthologs from human, yeast, and *Arabidopsis*, and found that SAE2 regions involved in E2 interactions exhibited a conservation degree from two- to six-fold lower than the conservation displayed by the SAE2 domains in which they are contained, the full UFD or full Cys domain, respectively (Supplemental Figure 2). This localized divergence suggests that these regions, which we have named LHEB1 and LHEB2 (low homology region involved in E2 binding 1 and 2), have optimized cognate interactions across evolution. From the E2 side, the region involved in SAE2 binding is better conserved across species and also participates in SUMO non-covalent interactions (Wang et al., 2010), which are necessary for polySUMO chain formation (Capili and Lima, 2007; Knipscheer et al., 2007; Castaño-Miquel et al., 2011). To avoid interfering with protein-protein interactions other than E1-E2 interactions, we designed a strategy based on SAE2^{UFDCt} domain engineering. The SAE2^{UFDCt} domain includes residues from Ser436 to Glu625. In SUMO conjugation assays *in vitro*, the *Arabidopsis* SAE2^{UFDCt} domain is essential for SUMO conjugation and, when included as an independent domain in the assays, the SAE2^{UFDCt} domain displayed the capacity to inhibit SUMO conjugation in a dose-dependent manner (Figure 1C and 1D). The SAE2^{UFDCt} domain was also competent to inhibit SUMOylation of SCE1, which further supports the role of the SAE2^{UFDCt} domain in the direct disruption of E1-E2 interactions (Supplemental Figure 4).

The SAE2^{UFDCt} LHEB2 Region Has a Major Role in SAE2^{UFDCt}–SCE1 Non-covalent Interactions

Previous structural studies suggested that yeast LHEB2 establishes hydrophobic and ionic interactions with Ubc9 (yeast SUMO E2 enzyme), which involve one Leu and two Asp residues, respectively (Wang et al., 2010). Due to the low homology between *Arabidopsis* and yeast LHEB2 regions (6% of sequence identity), it was not possible to unequivocally identify the corresponding functional residues in *Arabidopsis* SAE2. Instead, we performed comparative analyses of LHEB2 sequence conservation among plant SAE2 orthologs and their corresponding UFD domain assigned according to sequence homology. The identified SAE2^{UFD} sequences were realigned and the resulting alignment was used to perform phylogenetic analyses of the UFD (Supplemental Figure 3A) or the LHEB2 domain (Figure 2A) sequences. The resulting parsimony phylogenetic trees showed that the evolutionary relationships among the SAE2^{UFD} domain sequences were consistent with taxonomic lineages. On the contrary, when the evolutionary relationship between LHEB2 sequences was analyzed, the resulting clades were not consistent with taxonomic lineages (Supplemental Figure 3B and 3C), supporting the hypothesis that the LHEB2 domain has undergone higher diversification than the overall SAE2 sequence. The LHEB2 consensus sequence was determined for angiosperms, lower plants, and algae (Figure 2B), and their comparative analysis showed that the LHEB2 domain displayed differences in sequence length and composition among these evolutionary groups.

From the angiosperm LHEB2 consensus sequence, we selected hydrophobic and acidic amino acid residues that could potentially be involved in E2 binding according to previous reports in yeast (Wang et al., 2010) (Figure 2B and Supplemental Figure 2). To analyze the role of the selected residues in E2 binding, we introduced four single mutations into SAE2^{UFDCt}, L476A, L477A, D485A, and D486A, and tested their effect in SAE2^{UFDCt}–E2 interactions in pull-down assays *in vitro*. All SAE2^{UFDCt} mutant forms were impaired in E2 binding, although this defect was more prominent in L476A and D485A mutant forms (Figure 2C and 2D). These results were consistent with a major role of polar and hydrophobic interactions in E2 binding. Also, these results showed that amino acid residues in SAE2^{UFDCt} LHEB2 are crucial for establishing SUMO E1-E2 interactions.

Constitutive Expression of SAE2^{UFDCt} Domain Confers Attenuated Developmental Defects Displayed by SUMOylation-Impaired Plants

To test the capacity of the SAE2^{UFDCt} domain to inhibit SUMO conjugation *in vivo*, we generated transgenic plants expressing *Arabidopsis* SAE2^{UFDCt} domain under the control of the CaMV

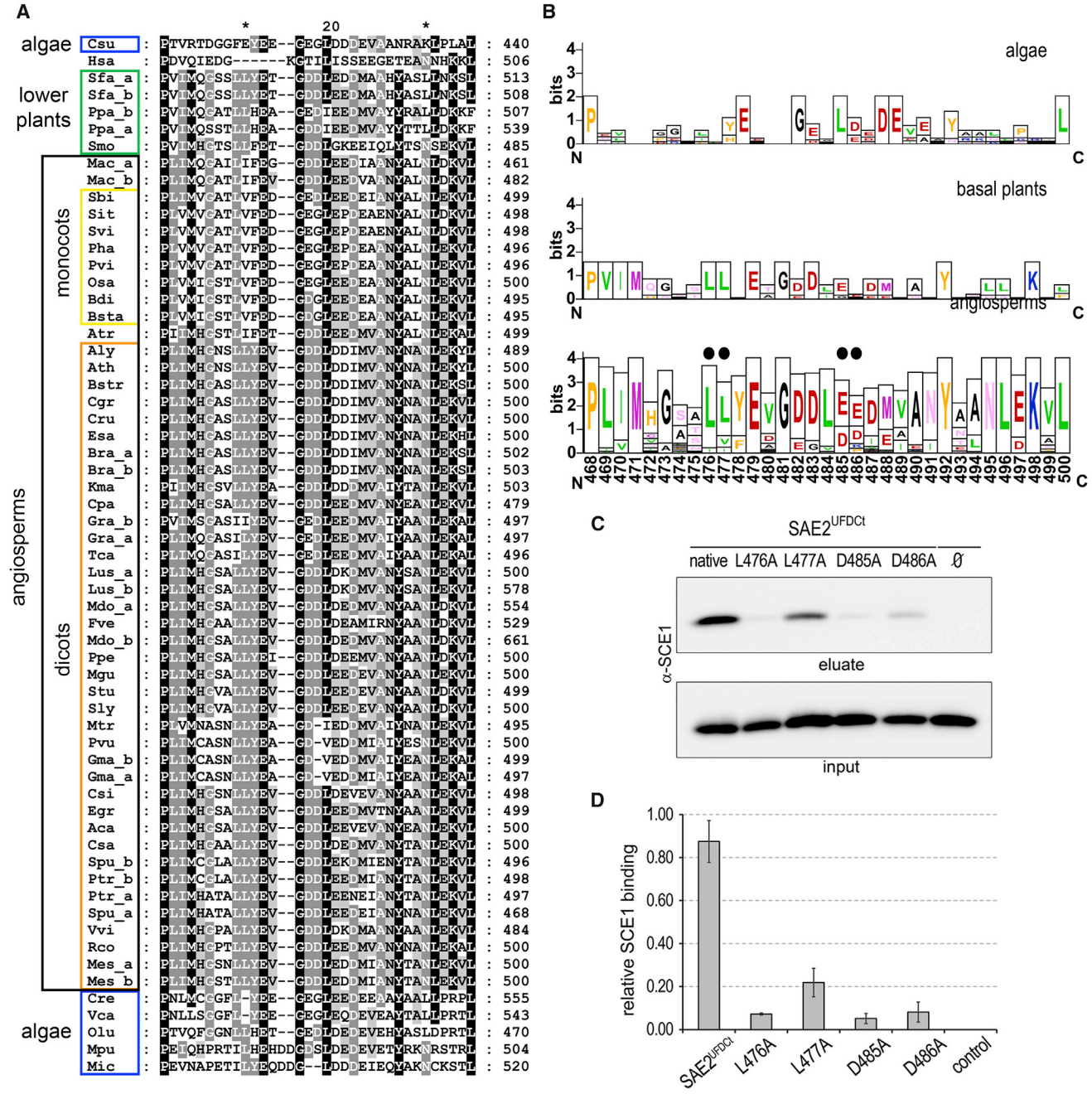

Figure 2. Molecular Analysis of SAE2^{UFDCt}-SCE1 Interactions.

(A) Viridiplantae (green algae and land plants) SAE2 LHEB2 sequence alignment. Sequence identity is indicated by black background and white letters (90%), gray background and white letters (70%), and light-gray background and black letters (50%). Gaps in the alignment due to insertions or deletions are indicated by dashed lines. Residue numbers are shown to the right side of the sequences. Sequence names correspond to the first letter of the genus followed by the two first letters of the species (e.g., *Arabidopsis th*aliana, *Ath*). Sequences are listed in Supplemental Table 1.

(B) Graphical representation of plant LHEB2 consensus sequence determined from dicot and monocot SAE2^{UFDCt} sequence alignment. The overall height of the stack indicates the sequence conservation at that position, while the height of symbols within the stack indicates the relative frequency of each amino acid at that position. Amino acids predicted to have a role in SAE2^{UFDCt}-E2 interactions are indicated by black dots.

(C) *In vitro* polyHis pull-down assay of *Arabidopsis* SCE1 using His:SAE2UFDCt or its mutant variants as a bait. Incubations in the absence of the bait were used as negative controls (Ø).

(D) Aliquots of input and eluate fractions were resolved by SDS–PAGE and SCE1 levels were analyzed by immunoblotting. Assays were performed in triplicates and relative SCE1 levels quantified. Average values and SE bars are plotted on the graph.

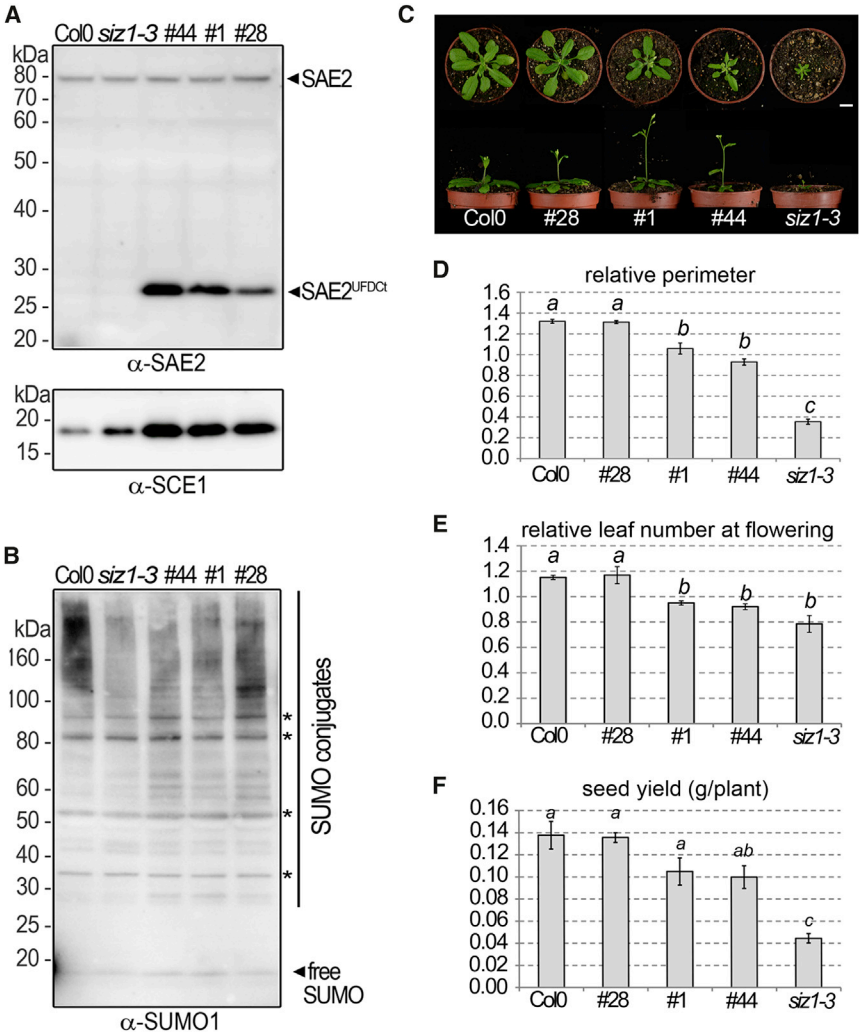

Figure 3. Effect of SAE2^{UFDCt} Expression in Endogenous SUMO Conjugation and Plant Development.

(A and B) Effect of SAE2^{UFDCt} expression on SUMO conjugates SAE2 and SCE1 levels. Total protein extracts from 4-day-old seedlings were resolved by SDS–PAGE and examined by immunoblot analysis with **(A)** anti-SAE2, anti-SCE1, and **(B)** anti-SUMO1 antibodies. Bands that are not significantly reduced in SUMOylation-deficient plants are indicated by asterisks.

(C) Developmental stage of 3-week-old plants grown under long-day conditions. Scale bar represents 1 cm. Top and lateral views of representative plants are shown.

(D) Rosette perimeter according to ellipse perimeter defined by the three most external leaf tips from each rosette. Average values and SEM from relative values obtained in four biological replicates are plotted on the graph.

(E) Rosette leaf number at flowering was scored when the inflorescence had reached 1 cm. Average values and SEM from relative values obtained in four biological replicates are plotted on the graph.

(F) Seeds were harvested from individual fully dried plants and their weight measured. Average values and SEM from relative values obtained in three biological replicates are plotted on the graph. *siz1-3* mutant was included as a control in all the analyses. *t*-Test was performed, and groups with the same letter denote no statistically significant differences between them ($p > 0.05$).

35S promoter. Among the obtained transgenic plants, three independent lines expressing from lower to higher levels of SAE2^{UFDCt}, #28, #1, and #44, were selected for further characterization (Figure 3A, top). In these plants, accumulation of SUMO conjugates was diminished in direct relation to SAE2^{UFDCt} expression levels (Figure 3B and Supplemental Figure 5). As controls, we included Columbia-0 (Col-0) and *siz1-3* mutant plants, which displayed the highest and the lowest SUMO conjugate accumulation levels among the analyzed lines, respectively. Remarkably, SCE1 levels were significantly increased in these plants (Figure 3A, bottom), and this increment was proportional to SAE2^{UFDCt} expression levels. In contrast, SAE2 endogenous levels were not altered. The analysis of mRNA SCE1 levels revealed no significant differences between SUMOylation-impaired plants and control Col-0 plants (Supplemental Figure 7), suggesting that regulation of endogenous SCE1 protein levels would involve a novel post-transcriptional mechanism.

The phenotypic analysis showed that SAE2^{UFDCt}-expressing plants displayed developmental alterations present in SUMOylation-deficient plants, such as reduced plant size (Figure 3C and 3D), early flowering (Figure 3E), and reduced seed yield (Figure 3F) (Lois, 2010). The extent of these alterations was consistent with a gradual SUMO conjugation inhibition between the different transgenic lines and was maintained through generations. In addition, SAE2^{UFDCt} expression impaired desiccation-induced SUMO conjugate accumulation and conferred plant susceptibility to drought (Supplemental Figure 6), both responses characteristic of the SUMO E3 ligase mutant *siz1-3* (Catala et al., 2007).

At the molecular level, we characterized the capacity of SAE2^{UFDCt} to interact with SCE1 as a mechanism of SUMO conjugation inhibition. In transient expression experiments in onion cells, SCE1 localized to the nucleus and the cytosol while the SAE2^{UFDCt} domain localized exclusively to the nucleus, which is consistent with the presence of a nuclear localization signal in the SAE2 C-terminal tail (Castaño-Miquel et al., 2013). When SAE2^{UFDCt} and SCE1 were co-expressed, SCE1 localized exclusively to the nucleus, suggesting that the SCE1 cytosolic fraction was recruited to the nucleus by SAE2^{UFDCt} (Figure 4A). To further test the SAE2^{UFDCt}–E2 interactions *in vivo*, we performed immunoprecipitation assays in protein extracts from line #44 of SAE2^{UFDCt}-expressing plants. The SUMO-E2-conjugating enzyme SCE1 was specifically co-immunoprecipitated when anti-SAE2 antibodies were used, but not in the presence of pre-immunization antibodies, further supporting that the SAE2^{UFDCt} domain is competent for E2 recruitment *in vivo* (Figure 4B).

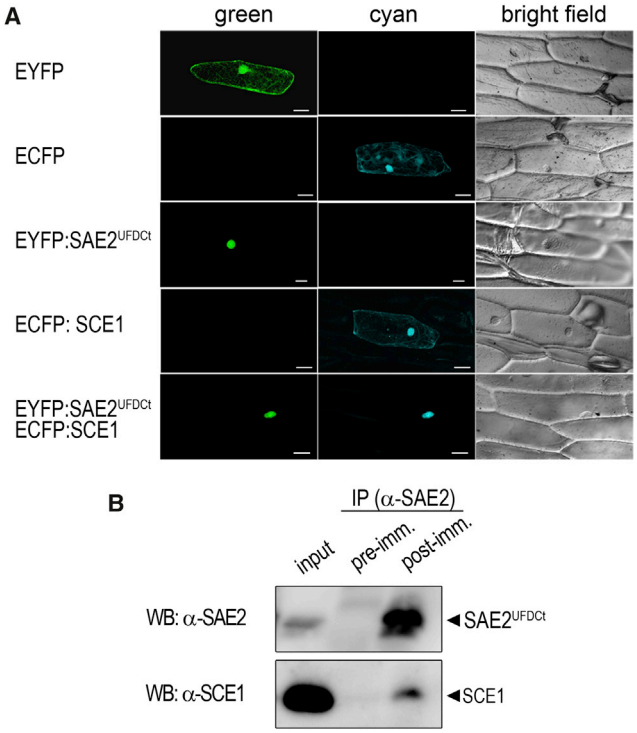

Figure 4. Analysis of SAE2^{UFDCt}–SCE1 Interactions *In Vivo*.
(A) SAE2^{UFDCt} and SCE1 co-localize in the nucleus of onion cells. SAE2^{UFDCt} fused to enhanced YFP (EYFP) and SCE1 fused to ECFP were transiently expressed in onion epidermal cells, individually or co-expressed. Cells expressing EYFP or ECFP were used as control. Light-transmission images of the fluorescent protein-expressing cells are shown next to the corresponding fluorescence image. Scale bars, 50 μm.
(B) Total protein extracts from *Arabidopsis* plants expressing the SAE2^{UFDCt} domain (line #44) were subjected to immunoprecipitation with pre-immune serum or SAE2 post-immunization serum. Input and immunoprecipitated protein fractions were analyzed by immunoblotting using anti-SAE2 or anti-SCE1 antibodies.

Plants with Impaired SUMOylation Exhibit Enhanced Susceptibility to Fungal Pathogen Infection

To further validate the developed strategy for inhibiting SUMO conjugation *in vivo*, we investigated a novel role of protein SUMOylation in plant defense against fungal pathogens. For this purpose, several *Arabidopsis* genotypes with altered SUMOylation activity were challenged with two different necrotrophic pathogens, namely *B. cinerea* and *P. cucumerina*. The selected plants accounted for increased SUMOylation, SUMO1-ox plants (Lois et al., 2003), and diminished SUMOylation, including SUMOylation-deficient SAE2^{UFDCt}-expressing plants lines #28, #1, and #44, and *siz1-3* mutant plants. The progress of diseases was macroscopically examined and compared with wild-type plants. Disease lesions caused by *B. cinerea* were first visible as discrete necrotic spots at 2 days post infection (dpi) in those lines impaired in SUMOylation, whereas in the wild-type and *SUM1*-ox leaves necrosis appeared later, at 3 dpi (Figure 5A). These lesions expanded and caused maceration on the inoculated leaves in the next few days, developing more quickly on the *siz1-3*- and the *SAE2^{UFDCt}*-expressing lines (Figure 5A). At 15 dpi, most of inoculated *siz1-3* mutant and transgenic plants from lines #1 and #44 were dead, whereas most of the wild-type, *SUM1*-ox, and line #28 plants remained alive and survived the disease under these experimental conditions (Figure 5B). These results suggest that protein SUMOylation is required for resistance to *B. cinerea* fungal infection. Similarly, the plants impaired in SUMOylation showed enhanced susceptibility to the fungal pathogen *P. cucumerina*, as they displayed necrosis on the majority of leaves at 7 dpi (Figure 5C) that expanded through the petioles and reached the vascular system, causing approximately 50% decay of plants at 10 dpi (Figure 5D). This phenotype differed from the moderate susceptibility shown by the wild-type and *SUM1*-ox plants, in which necrotic spots in most of the leaves were observed, although complete necrosis only developed in basal leaves and most of the inoculated plants survived (Figure 5C and 5D). In these experiments, the *agb1-1* mutant (Llorente et al., 2005), which displays an enhanced susceptibility to *P. cucumerina*, was used as positive control of fungal infection. These macroscopic disease symptoms were associated with a higher fungal growth on *siz1-3* or *SAE2^{UFDCt}* leaves, as revealed by trypan blue staining of fungal hyphae (Figure 5E). The SUMOylation-deficient leaves and the *agb1-1* mutant supported an increased fungal growth, consistent with the displayed plant susceptibility. The *SUM1*-ox and wild-type plants with high and basal SUMOylation profiles, respectively, showed moderate susceptibility, whereas the *SAE2^{UFDCt}* lines and *siz1-3* mutant plants with reduced SUMOylation conjugates showed high susceptibility to *P. cucumerina* (Figure 5F).

To better understand the requirement of SUMOylation for necrotrophic pathogen resistance, we analyzed the molecular dynamics of SUMO, free and conjugated, and two members of the SUMOylation machinery, the SUMO-activating enzyme large subunit SAE2 and the SUMO-conjugating enzyme SCE1, during *P. cucumerina* infection of wild-type Col-0 plants. At 3 hours post infection (hpi), a transient and significant increment in SUMO conjugates was observed, followed by a gradual reduction of SUMO conjugates reaching a 50% reduction at 48 hpi, which did not correlate with an accumulation of free SUMO. On the contrary, free SUMO levels were also reduced during infection (Figure 6A and 6C), indicating that the reduction of SUMO conjugates is not a consequence of active deconjugation. Similarly, SAE2 and SCE1 protein levels diminished during infection, although with slightly different dynamics. SCE1 levels were gradually reduced, whereas SAE2 levels were maintained up to 24 hpi and then reduced at 48 hpi (Figure 6A, 6D, and 6E). After 7 dpi, dead plants were clearly observed (Supplemental Figure 8). The analysis of mRNA SUMO1, SAE2, and SCE1 levels did not reveal fluctuations that would account for the reduction in protein levels (Figure 6B). These results suggest that reduction of SUMO, SAE2, and SCE1 protein levels in response to necrotrophic fungal infection is post-transcriptionally controlled.

DISCUSSION

Taking advantage of the highly specific protein–protein interactions among cognate enzymes that mediate SUMO conjugation to substrates, we have developed a novel strategy for achieving inhibition of SUMO conjugation *in vivo* based on disruption of SUMO E1–E2 interactions. We have validated this strategy for uncovering a novel role of SUMO conjugation in defense responses to necrotrophic fungal pathogens.

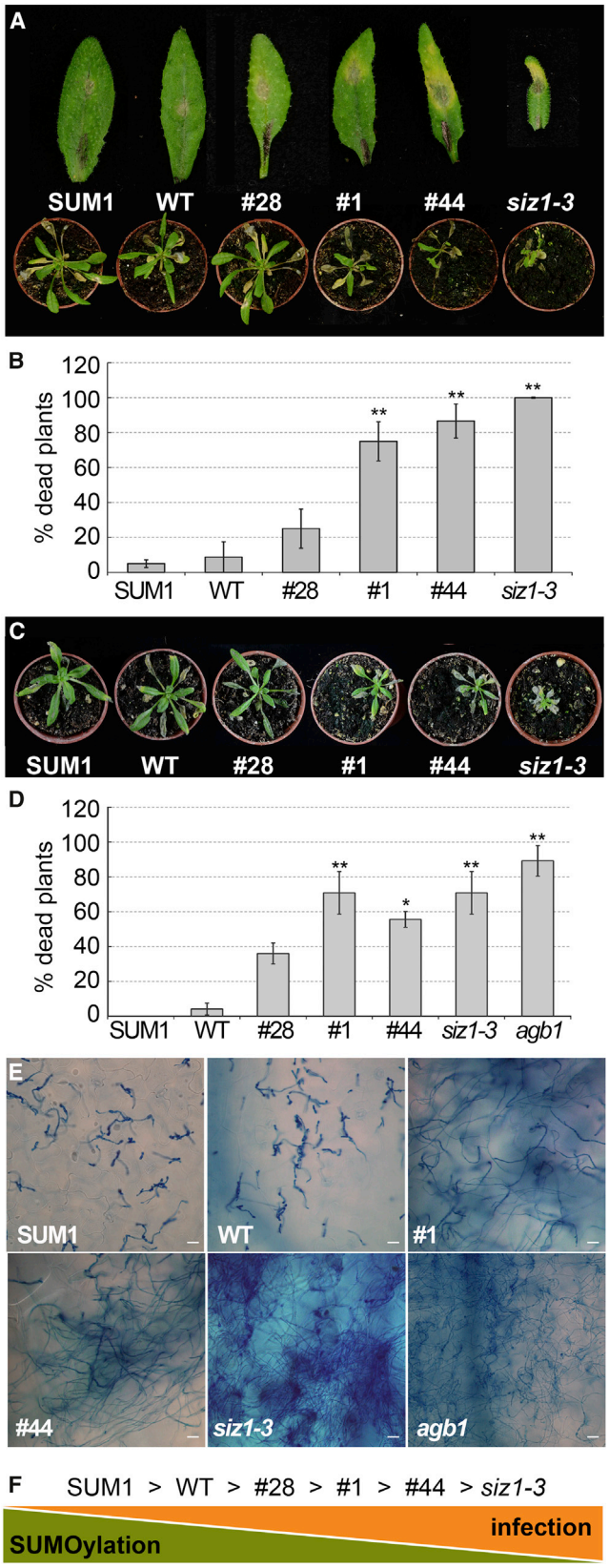

Figure 5. Sumoylation Is Required for Fungal Resistance.
Susceptibility of the indicated *Arabidopsis* genotypes with altered SUMOylation activity to *Botrytis cinerea* **(A and B)** and *Plectosphaerella cucumerina* **(C–E)** infection.

Structure-Based SUMO Conjugation Inhibition

Since SUMOylation is an essential process, the use of knockout mutants affecting the first steps in the SUMO conjugation pathway, such as the E1-activating or the E2-conjugating enzymes, is compromised. As a result, the use of knockout mutants has been limited to the study of specific E3 ligase-dependent functions, such as SIZ1 or MMS21, which are the only SUMO E3 ligases described in *Arabidopsis*. Null *siz1* and *mms21* mutant plants display dramatic pleiotropic growth defects (Ishida et al., 2009; Miura et al., 2010), which could raise concerns about the direct role of SUMO in the reported biological functions. In addition, the dependence of the *siz1* phenotype on growth conditions has generated contradictory observations regarding its role in drought responses (Catala et al., 2007; Miura et al., 2013), accentuating the need for alternative genetic tools. The strategy that we have developed renders plants without compromised viability and facilitates the study of physiological processes over a range of SUMOylation inhibition, establishing dose-dependent responses. Both aspects constitute an advantage over the use of null E3 ligase mutants.

Previous attempts aimed to inhibit *in vivo* SUMOylation by expressing a SUMO E2-inactive mutant, but resulted in transgene silencing after few generations (Lois et al., 2003; Tomanov et al., 2013). In contrast, the expression of the SAE2^{UFDCt} domain is maintained through generations. In addition, inhibition of protein functions has some advantages over applying RNA interference approaches such as avoiding off-target effects (Jackson and Linsley, 2010), and it is easier to implement in species with high genome complexity, such as some crops, than approaches involving multiple knockout or knockdown mutant generation. Considering the mentioned aspects, SAE2^{UFDCt} expression is a reliable and novel approach to inhibit SUMO conjugation *in vivo* that could contribute to accelerating our knowledge of how SUMO regulates traits affecting productivity of important crops.

New Mechanistic Insights into *In Vivo* SUMO Conjugation

To our knowledge, this is the first report describing that the disruption of SUMO E1–E2 interactions is a valid strategy for inhibiting SUMO conjugation *in vivo*, and supports a major role

(A) Top: representative leaves detached from drop inoculated plants (10^6 spores/ml) with early disease symptoms at 3 dpi. Bottom: phenotype of plants at 7 dpi that were inoculated on four leaves per plant.
(B) Percentage of dead plants at 15 dpi. Average values and SEM were calculated from five independent assays in which eight plants per genotype were analyzed.
(C) Phenotypical appearance of representative plants at 7 days after spray inoculation with a 10^5 spores/ml suspension.
(D) Percentage of dead plans at 10 dpi. Average values and SEM were calculated from three independent assays in which eight plants per genotype were analyzed.
(E) Trypan blue staining of *P. cucumerina* fungal hyphae growing on leaves at 3 dpi. Scale bars, 20 μm.
(F) Representative scheme of protein SUMOylation levels and fungal infection susceptibility.
Asterisks denote statistically significant differences with wild-type plants (Tukey's test, *$p < 0.05$, **$p < 0.01$).

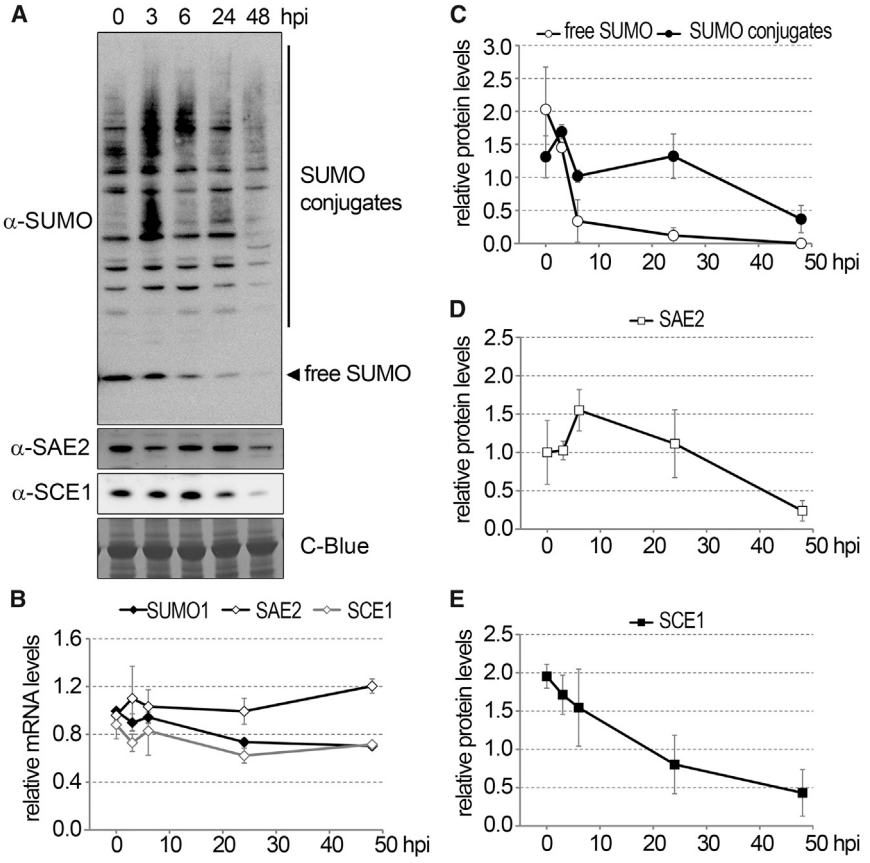

Figure 6. SUMO Conjugates and SUMO Conjugation Machinery Components SAE2 and SCE1 Protein Levels Diminish during Fungal Infection.

(A) Total protein extracts from 21-day-old seedlings, before infection (0) or after 3, 6, 24, and 48 hpi (hours post infection) were resolved by SDS–PAGE and examined by immunoblot analysis with anti-SUMO1, anti-SAE2, and anti-SCE1 antibodies.

(B) mRNA levels corresponding to SUMO1, E1-activating enzyme large subunit (SAE2), and E2-conjugating enzyme (SCE1) were quantified by qPCR. Collected data were normalized by using AtUBC21 as a reference gene.

(C–E) Relative protein levels were quantified from the same biological samples as in **(B)** and average values and SEM were plotted on the corresponding graphs. Quantifications were performed from two or three biological replicates.

for the SAE2^{UFDCt} domain in E2 recruitment *in vivo*. Disruption of protein–protein interactions potentially offers advantages over single enzyme inhibition related to increased affinity and specificity (Zinzalla, 2013). Accordingly, the low conservation displayed by the LHEB2 sequences suggests that these regions have evolved to optimize E1–E2 cognate interactions. Supporting this hypothesis, previous studies performed by us and others showed that the *in vitro* efficiency of the human SUMO conjugation system was dramatically reduced when the human E2-conjugating enzyme was replaced by the *Arabidopsis* (Lois et al., 2003) or *Plasmodium falciparum* (Reiter et al., 2013) SUMO E2 orthologs. Also, as result of this divergence the identification of specific amino acids displaying a major contribution to these interactions is not possible by sequence homology between evolutionary distant organisms, such as yeast and plants. By using mutagenesis analysis, we have identified residues necessary for SAE2^{UFD}–E2 interactions that are present with a high frequency in the angiosperm SAE2 sequences analyzed, but not in lower plants, consistent with the proposed higher divergence rate of this region.

In addition, we have uncovered a novel post-transcriptional regulation of SUMO E2 levels, which accumulate in direct relation to the SAE2^{UFDCt} expression levels. Previous studies reported an accumulation of the E2 in *siz1* mutant plants and suggested the existence of a compensatory mechanism that was not analyzed (Saracco et al., 2007). We have observed similar E2 accumulation in *siz1* mutant plants, but this accumulation was much higher in SAE2^{UFDCt}-expressing plants even though they displayed less dramatic defects in SUMO conjugate accumulation than in *siz1* mutant plants. This is particularly evident in the case of the transgenic line expressing the lowest SAE2^{UFDCt} levels, line #28, which had a minor effect on SUMO conjugate accumulation; consequently, plants did not display obvious developmental defects under standard growth conditions. These results provide evidence for the existence of an unknown *in vivo* SUMOylation regulation mechanism based on the control of E2 levels. We speculate that the SCE1–SAE2^{UFDCt} complex could mediate SCE1 stabilization. *In planta*, such mechanisms could facilitate the coordination between E1 and E2 levels to modulate SUMO conjugation rate.

SUMOylation Is Required for Resistance to Plant Necrotrophic Fungal Pathogens

In recent years post-translational modification mechanisms have emerged as key players in the plant defense responses to pathogens. The role of phosphorylation, ubiquitination, SUMOylation, nitrosylation, and glycosylation has been described in plant immunity (Lee et al., 2007; Stulemeijer and Joosten, 2008). Since previous studies did not identify alterations in *siz1* mutant plant susceptibility to necrotrophic pathogens, we evaluated a potential role of SUMO in this process that could potentially be SIZ1 independent. We found that transgenic plants expressing the SAE2^{UFDCt} domain displayed increased sensitivity to the tested fungi. Surprisingly, when we included *siz1* mutant plants in the assays, we observed that they also displayed sensitivity to necrotrophic fungal pathogens. Response variability of *siz1* mutant plants upon stress was previously observed in drought tolerance studies (Catala et al., 2007; Miura et al., 2013), stressing the need for alternative and more reliable approaches to study the role of SUMOylation in plants, such as the strategy described here. In fact, SAE2^{UFDCt}-expressing plants also displayed increased drought sensitivity, supporting the findings of Catala et al. (2007).

Defense responses regulated by the salicylic acid-dependent pathway and associated with programmed cell death, which are effective against biotrophic pathogens, benefit necrotrophic pathogens. The null *siz1* mutant plants are characterized by high contents of salicylic acid, which results in higher expression of PR genes inducing a constitutive systemic acquired resistance, leading to an increased resistance to the bacterial pathogen *Pseudomonas syrinage* pv. *tomato* (*Pst*) (Lee et al., 2007; van den Burg et al., 2010). Therefore, the *siz1* susceptibility to necrotrophic pathogens that we observed is consistent with salicylic acid accumulation in these plants.

To further understand the role of SUMOylation in pathogen defense, we determined protein dynamics of SUMO conjugation machinery members, SUMO E1-activating enzyme large subunit, E2-conjugating enzyme, and free and conjugated SUMO, during the first 48 hpi, when physical damage was not observed. Although the different components follow distinct dynamics, at 48 hpi a general depletion of the SUMOylation system was observed, which did not correlate with significant alterations in mRNA levels, suggesting the existence of a post-transcriptional regulation. Since SUMOylation inhibition results in cell death (Miura et al., 2010), it is plausible that necrotrophic fungi could induce SUMOylation machinery depletion as a mechanism of pathogenicity. Supporting this hypothesis, the role of some bacterial pathogen effectors targeting the host SUMOylation machinery is well described. As such, the *Xanthomonas campestris* effectors XopD and AvrXv4 act as SUMO proteases (Chosed et al., 2007), resulting in the disruption of SUMO homeostasis in the cell (Hotson and Mudgett, 2004; Roden et al., 2004), which favors infection progression. In viral infections, the essential proteins for viral replication AL1 and REP interact with SUMO E2-conjugation enzyme, altering the cell SUMO conjugation capacity (Castillo et al., 2004; Sanchez-Duran et al., 2011). This manipulation of SUMOylation machinery by pathogens is a strategy also present in animal viruses and bacteria (Boggio et al., 2007; Ribet et al., 2010; Beyer et al., 2015). The existence of similar strategies used by fungi during host infections remains to be elucidated.

Overall, we have validated the disruption of SUMO E1 and E2 interactions as a reliable strategy for inhibiting SUMO conjugation *in vivo*, which could be applied to accelerate the understanding of SUMOylation in organisms for which genetic tools are not available, such as economically relevant crops. Also, this validation constitutes a starting point from which to develop novel agrochemicals for selective modulation of plant stress responses such as plant immunity. Finally, we have shown the advantage of this strategy over the use of null mutants, which sometimes deliver contradictory results, by identifying a novel role of SUMO in defense responses against necrotrophic fungal pathogens. Additional studies will be necessary to elucidate the molecular mechanisms involved in SUMO conjugation machinery depletion during fungal infection.

METHODS

Plant Material and Growth Conditions

For *in vitro* cultures, seeds were stratified for 3 days, plated on Murashige and Skoog salts (pH 5.7) (Duchefa), supplemented with 0.8% BactoAgar (Difco), and transferred to a tissue culture room in a long-day (LD) photoperiod (16 h light/8 h dark) at 22°C. For soil cultures, plants were grown in growth chambers under LD photoperiod at 22°C. For immunoprecipitation assays, seedlings of SAE2^{UFDCt} expressing line #44 were germinated and grown in Gamborg liquid medium for 11 days in constant agitation (120 rpm) under LD photoperiod culture room. Plants were immediately frozen with N_2 and stored at −80°C.

In Vitro SUMO Conjugation

A detailed protocol for reconstituting an *in vitro* SUMO conjugation assay covering all steps from protein preparation to assay development and kinetics quantification is described in Castaño-Miquel and Lois (2016). In brief, in conjugation assays we used the C-terminal tail of the *Arabidopsis* Catalase 3 (419–472) fused to GST, GST:AtCAT3Ct as a substrate. Reactions were carried out at 37°C in 25-μL reaction mixtures containing 1 mM ATP, 50 mM NaCl, 20 mM HEPES (pH 7.5), 0.1% Tween 20, 5 mM $MgCl_2$, 0.1 mM DTT, 2 μM SUMO, 0.5 μM AtSAE2/AtSAE1a, 0.5 μM AtSCE1, and 5 μM GST-AtCAT3Ct. After the specified incubation time, reactions were stopped by the addition of protein-loading buffer, incubated at 70°C for 10 min, and 10-μL aliquots were resolved by SDS–PAGE. Reaction products were detected by immunoblot analysis with anti-GST polyclonal antibodies (Sigma, G7781). Luminescence signal generated by ECL Prime assay (GE Healthcare) was captured with a CCD camera (LAS4000, Fujifilm) and quantified with Multigauge software (Fujifilm). Each data point was normalized to the average of all data points obtained from each analyzed membrane to remove variability resulting from antibody incubations and time-exposure differences. The normalized values were used to calculate the corresponding slopes (relative luminescence signal versus time). The average slope from at least three independent experiments is shown.

In Vitro Pull-Down Assay

One hundred μM His:AtSAE2^{UFDCt} or its mutant variants L476A, L477A, D485A, and D486A, and 25 μM AtSCE1 were incubated in 40 μL of binding buffer (50 mM Tris [pH 8.0], 150 mM NaCl, and 20 mM imidazole) for 1 h at 4°C. Next, 10 μL of Ni^{2+}-IMAC-Sepharose resin was added to the binding mixture and incubated for 30 min at 4°C. The binding mixture was transferred to micro bio-spin chromatography columns (Bio-Rad, 732–6203) and the resin was washed three times with 20 μL of binding buffer and a final wash of 40 μL of binding buffer. The proteins bound to the resin were eluted with 20 μL of binding buffer containing 300 mM imidazole. 0.5 μL of the input and 1 μL of the eluate fractions, respectively, were separated by SDS–PAGE and subjected to immunoblot analysis with anti-SCE1 antibodies.

Transient Expression of Fluorescent Protein Fusions in Onion Cells

SAE2^{UFDCt} and SCE1 were fused in frame to the 3′ end of the coding sequences of yellow fluorescent protein (YFP) or cyan fluorescent protein (CFP), respectively, downstream of the 35S constitutive promoter. Onion epidermal cells were bombarded with 5 μg of each DNA construct using a helium biolistic gun (Bio-Rad). Treated epidermal cells were kept in the dark at room temperature for 16 h before analysis by confocal microscopy (Confocal Olympus FV 1000). YFP was excited with a 515-nm argon laser and images collected with a 550- to 630-nm range. CFP was excited with a 405-nm argon laser and images collected in the 460- to 500-nm range. Imaging of YFP and CFP imaging and transmissible light image collection were performed sequentially. Samples were scanned with the z-stack mode and image stacks projection was calculated with ImageJ software (Rasband, 1997-2009).

Protein Extraction and Immunoblot

Anti-SUMO1/2, anti-SAE2, and anti-SCE1 polyclonal antisera were generated previously (Castaño-Miquel et al., 2011). Plant tissue was ground in liquid nitrogen and proteins extracted with 50 mM Tris–HCl (pH 8), 150 mM NaCl, 0.2% Triton X-100, 1 mM PMSF, 1 μg/ml pepstatin, 1 μg/ml leupeptin, 2 mM *N*-ethylmaleimide, 10 mM iodoacetamide, and

5 mM EDTA. Total protein (18 μg) was resolved under reducing conditions by using SDS–polyacrylamide gels and NuPage Novex 4%–12% Bis/Tris gels (Invitrogen). Proteins were transferred onto polyvinylidene difluoride membranes (Millipore) and incubated overnight with primary antibody, followed by secondary antibody incubation with peroxidase-conjugated anti-rabbit (GE Healthcare), for 1 h at room temperature in TBST buffer (20 mM Tris–HCl (pH 7.6), 20 mM NaCl, 0.1% [v/v] Tween 20) supplemented with 3% non-fat dry milk. Peroxidase activity was developed in ECL Plus reagent (GE Healthcare) and chemiluminescence signal captured with an LAS-4000 imaging system (Fujifilm). For SUMO conjugate quantifications, using Multigauge v.3 (Fujifilm), the region of interest (ROI) was defined by a rectangle enclosing all detected bands above free SUMO in each lane. The same ROI size was used for quantifying SUMO conjugates from each sample lane and the membrane background. Average values were calculated as described in Castaño-Miquel and Lois (2016).

Phylogenetic Analyses

We searched Phytozome v.11 for *Arabidopsis* SAE2 homologs and retrieved 100 sequences. Before performing comprehensive homology analysis, incomplete sequences were removed. When different versions of the same gene were found, we retained the version containing all the canonical SAE2 functional regions for the comparative analysis. The remaining 60 SAE2 homolog proteins from 54 plant species were aligned using the OMEGA Clustal software (http://www.ebi.ac.uk/Tools/msa/clustalo/) and the human SAE2 as outlier. Phylogenetic analysis was performed using Seaview software. Consensus sequences were calculated using WebLogo software (http://weblogo.berkeley.edu/) (Crooks et al., 2004). Multiple sequence alignments were edited, analyzed, and shaded using GeneDoc (Nicholas and Nicholas, 1997).

Immunoprecipitation Assays

One gram of 11-day old *Arabidopsis* seedlings was ground and homogenized in 2 ml of immunoprecipitation (IP) buffer (50 mM Tris–HCl [pH 7.5], 100 mM NaCl, 0.2% Triton X-100, 1 mM DTT, 1 μg/ml pepstatin, 1 μg/ml leupeptin, 2 mM *N*-ethylmaleimide, 10 mM iodoacetamide, and 5 mM EDTA), incubated for 30 min rotating at 4°C, and centrifuged at 14 000 *g* for 20 min at 4°C. Supernatants were recovered and concentrated with centrifugal filters (Amicon Ultra-15 10 kDa) and subsequently quantified using the Bradford assay (Bio-Rad Protein Assay). Total protein (12 mg) was incubated for 3 h at 4°C on a rotator in the presence of 30 μL of SAE2 polyclonal antiserum, or 90 μL of the corresponding pre-immunization serum, and 50 μL of Protein A magnetic beads (Surebeads, Bio-Rad). After three washes with IP buffer, immunoprecipitated proteins were eluted by boiling at 100°C in Laemmli buffer and analyzed by immunoblotting using anti-SAE2 and anti-SCE1 antibodies. As control, 5 μg of input fractions was also analyzed.

RNA Extraction and Quantitative Real-Time RT–PCR

Total RNA from plant tissues was extracted using the Maxwell 16 LEV simplyRNA Tissue Kit (Promega, WI, USA) according to the manufacturer's instructions. The Superscript VILO kit (Invitrogen, MA, USA) was used to generate cDNA according to the manufacturer's instructions, using 1.4 μg of total RNA. The relative mRNA abundance was evaluated via quantitative RT–PCR in a total reaction volume of 20 μL using LightCycler 480 SYBR Green I Master (Roche, Basel, Switzerland) on a LightCycler 480 Real-Time PCR System (Roche, Basel, Switzerland) with 0.3 μM of each specific sense and anti-sense primers. Two or three independent biological replicates of each sample, as stated in the text, and three technical replicates of each biological replicate were performed and the mean values were considered for further calculations. The relative transcript level was determined for each sample and normalized using *UBC21* or *PR65* as stated. Primer sequences used in the qPCR experiments are described in Supplemental Table 2.

Infection Assays

The *B. cinerea* and *P. cucumerina* fungal strains, as well as the *Arabidopsis* mutant *agb1-1* showing high susceptibility to *P. cucumerina* infection (Delgado-Cerezo et al., 2012), were provided by Dr. A. Molina (CBGP, Spain). Plants were grown in a phytochamber on a sterilized mixture of soil and vermiculite (3:1) during 4 weeks under a 12 h light/12 h dark photoperiod at 22°C prior to inoculation. Inoculated plants were kept under high humidity in covered trays. *B. cinerea* inoculations were performed by placing spore suspension drops (10^6 spores/ml) on *Arabidopsis* leaves (four leaves per plant). *P. cucumerina* inoculations were performed by spraying plants with spore suspensions (10^5 spores/ml). At least eight plants per genotype were inoculated in a minimum of two or three independent assays. Disease progression was followed by visual inspection. Fungal growth was visualized by trypan blue staining of leaves at 2 and 3 dpi as reported (Epple et al., 1997), and bright field images were obtained on a Zeiss Axiophot microscope.

ACCESSION NUMBERS

Assigned accession numbers for the genes used in this work are as follows: At5g55160 (SUMO2), At2g21470 (SAE2), At4g24940 (SAE1a), At3g57870 (SCE1), and At1g13320 (PR65).

SUPPLEMENTAL INFORMATION

Supplemental Information is available at *Molecular Plant Online*.

FUNDING

This work was supported by the European Research Council (ERC-2007-StG-205927) and the Spanish Ministry of Science (BIO2008-01495). L.C.-M., I.T., A.P., S.M., and N.R. were supported by research contracts through the CRAG. A.M. and J.S. were supported by predoctoral fellowships, Spanish Ministry of Education, Culture and Sport (FPU12/05292) and Ministry of Education and Science (BES-2005-6843), respectively, and A.L.S. was supported by Beatriu de Pinós post-doctoral grant of the Generalitat de Catalunya (2013 BP_B 00182). We also thank the Generalitat de Catalunya (Xarxa de Referència en Biotecnologia and 2009SGR 09626) for substantial support.

AUTHOR CONTRIBUTIONS

L.C.-M., A.M., I.T., A.P., B.N.T., J.S., A.L.S., N.R., G.L.V., S.M., M.C., and L.M.L. performed experiments. L.C.-M., A.M., I.T., A.P., A.L.S., S.M., M.C., and L.M.L. designed experiments. M.C. supervised experiments involving fungal infections. L.M.L. supervised and led the project. M.C. and L.M.L. wrote the manuscript. L.C.-M., A.M., I.T., A.P., A.L.S., S.M., M.C., and L.M.L. discussed and checked the manuscript. All authors contributed to the analysis of the data and approved the manuscript.

ACKNOWLEDGMENTS

We thank the technical support from members of the Greenhouse and Microscopy facilities at CRAG. We greatly thank Cristina Cañadas for technical support at the L.M.L. laboratory. We thank Christopher D. Lima for critical reading of the manuscript. No conflict of interest declared.

Received: October 1, 2016
Revised: January 16, 2017
Accepted: January 19, 2017
Published: February 10, 2017

REFERENCES

Beyer, A.R., Truchan, H.K., May, L.J., Walker, N.J., Borjesson, D.L., and Carlyon, J.A. (2015). The *Anaplasma phagocytophilum* effector AmpA hijacks host cell SUMOylation. Cell. Microbiol. **17**:504–519.

Boggio, R., Passafaro, A., and Chiocca, S. (2007). Targeting SUMO E1 to ubiquitin ligases: a viral strategy to counteract sumoylation. J. Biol. Chem. **282**:15376–15382.

Capili, A.D., and Lima, C.D. (2007). Structure and analysis of a complex between SUMO and Ubc9 illustrates features of a conserved E2-Ubl interaction. J. Mol. Biol. **369**:608–618.

Castaño-Miquel, L., and Lois, L.M. (2016). Kinetic analysis of plant SUMO conjugation machinery. In Plant Proteostasis: Methods and Protocols, L.M. Lois and R. Matthiesen, eds. (New York: Humana Press), pp. 107–123.

Castaño-Miquel, L., Seguí, J., and Lois, L.M. (2011). Distinctive properties of *Arabidopsis* SUMO paralogues support the in vivo predominant role of AtSUMO1/2 isoforms. Biochem. J. **436**:581–590.

Castaño-Miquel, L., Seguí, J., Manrique, S., Teixeira, I., Carretero-Paulet, L., Atencio, F., and Lois, L.M. (2013). Diversification of SUMO-activating enzyme in *Arabidopsis*: implications in SUMO conjugation. Mol. Plant **6**:1646–1660.

Castillo, A.G., Kong, L.J., Hanley-Bowdoin, L., and Bejarano, E.R. (2004). Interaction between a geminivirus replication protein and the plant sumoylation system. J. Virol. **78**:2758–2769.

Catala, R., Ouyang, J., Abreu, I.A., Hu, Y., Seo, H., Zhang, X., and Chua, N.H. (2007). The *Arabidopsis* E3 SUMO ligase SIZ1 regulates plant growth and drought responses. Plant Cell **19**:2952–2966.

Chosed, R., Tomchick, D.R., Brautigam, C.A., Mukherjee, S., Negi, V.S., Machius, M., and Orth, K. (2007). Structural analysis of *Xanthomonas* XopD provides insights into substrate specificity of ubiquitin-like protein proteases. J. Biol. Chem. **282**:6773–6782.

Conti, L., Nelis, S., Zhang, C.J., Woodcock, A., Swarup, R., Galbiati, M., Tonelli, C., Napier, R., Hedden, P., Bennett, M., et al. (2014). Small ubiquitin-like modifier protein SUMO enables plants to control growth independently of the phytohormone gibberellin. Dev. Cell **28**:102–110.

Crooks, G.E., Hon, G., Chandonia, J.M., and Brenner, S.E. (2004). WebLogo: a sequence logo generator. Genome Res. **14**:1188–1190.

Delgado-Cerezo, M., Sanchez-Rodriguez, C., Escudero, V., Miedes, E., Fernandez, P.V., Jorda, L., Hernandez-Blanco, C., Sanchez-Vallet, A., Bednarek, P., Schulze-Lefert, P., et al. (2012). Arabidopsis heterotrimeric G-protein regulates cell wall defense and resistance to necrotrophic fungi. Mol. Plant **5**:98–114.

Epple, P., Apel, K., and Bohlmann, H. (1997). Overexpression of an endogenous thionin enhances resistance of Arabidopsis against Fusarium oxysporum. Plant Cell **9**:509–520.

Gareau, J.R., and Lima, C.D. (2010). The SUMO pathway: emerging mechanisms that shape specificity, conjugation and recognition. Nat. Rev. Mol. Cell Biol. **11**:861–871.

Glazebrook, J. (2005). Contrasting mechanisms of defense against biotrophic and necrotrophic pathogens. Annu. Rev. Phytopathol. **43**:205–227.

Hotson, A., and Mudgett, M.B. (2004). Cysteine proteases in phytopathogenic bacteria: identification of plant targets and activation of innate immunity. Curr. Opin. Plant Biol. **7**:384–390.

Huang, L., Yang, S., Zhang, S., Liu, M., Lai, J., Qi, Y., Shi, S., Wang, J., Wang, Y., Xie, Q., et al. (2009). The *Arabidopsis* SUMO E3 ligase AtMMS21, a homologue of NSE2/MMS21, regulates cell proliferation in the root. Plant J. **60**:666–678.

Ishida, T., Fujiwara, S., Miura, K., Stacey, N., Yoshimura, M., Schneider, K., Adachi, S., Minamisawa, K., Umeda, M., and Sugimoto, K. (2009). SUMO E3 ligase high PLOIDY2 regulates endocycle onset and meristem maintenance in *Arabidopsis*. Plant Cell **21**:1–14.

Jackson, A.L., and Linsley, P.S. (2010). Recognizing and avoiding siRNA off-target effects for target identification and therapeutic application. Nat. Rev. Drug Discov. **9**:57–67.

Knipscheer, P., van Dijk, W.J., Olsen, J.V., Mann, M., and Sixma, T.K. (2007). Noncovalent interaction between Ubc9 and SUMO promotes SUMO chain formation. EMBO J. **26**:2797–2807.

Lee, I., and Schindelin, H. (2008). Structural insights into E1-catalyzed ubiquitin activation and transfer to conjugating enzymes. Cell **134**:268–278.

Lee, J., Nam, J., Park, H.C., Na, G., Miura, K., Jin, J.B., Yoo, C.Y., Baek, D., Kim, D.H., Jeong, J.C., et al. (2007). Salicylic acid-mediated innate immunity in *Arabidopsis* is regulated by SIZ1 SUMO E3 ligase. Plant J. **49**:79–90.

Lois, L.M. (2010). Diversity of the SUMOylation machinery in plants. Biochem. Soc. Trans. **38**:60–64.

Lois, L.M., and Lima, C.D. (2005). Structures of the SUMO E1 provide mechanistic insights into SUMO activation and E2 recruitment to E1. EMBO J. **24**:439–451.

Lois, L.M., Lima, C.D., and Chua, N.H. (2003). Small ubiquitin-like modifier modulates abscisic acid signaling in *Arabidopsis*. Plant Cell **15**:1347–1359.

Llorente, F., Alonso-Blanco, C., Sanchez-Rodriguez, C., Jorda, L., and Molina, A. (2005). ERECTA receptor-like kinase and heterotrimeric G protein from *Arabidopsis* are required for resistance to the necrotrophic fungus *Plectosphaerella cucumerina*. Plant J. **43**:165–180.

Mengiste, T. (2012). Plant immunity to necrotrophs. Annu. Rev. Phytopathol. **50**:267–294.

Miura, K., Rus, A., Sharkhuu, A., Yokoi, S., Karthikeyan, A.S., Raghothama, K.G., Baek, D., Koo, Y.D., Jin, J.B., Bressan, R.A., et al. (2005). The *Arabidopsis* SUMO E3 ligase SIZ1 controls phosphate deficiency responses. Proc. Natl. Acad. Sci. USA **102**:7760–7765.

Miura, K., Lee, J., Jin, J.B., Yoo, C.Y., Miura, T., and Hasegawa, P.M. (2009). Sumoylation of ABI5 by the *Arabidopsis* SUMO E3 ligase SIZ1 negatively regulates abscisic acid signaling. Proc. Natl. Acad. Sci. USA **106**:5418–5423.

Miura, K., Lee, J., Miura, T., and Hasegawa, P.M. (2010). SIZ1 controls cell growth and plant development in *Arabidopsis* through salicylic acid. Plant Cell Physiol. **51**:103–113.

Miura, K., Sato, A., Ohta, M., and Furukawa, J. (2011). Increased tolerance to salt stress in the phosphate-accumulating *Arabidopsis* mutants *siz1* and *pho2*. Planta **234**:1191–1199.

Miura, K., Okamoto, H., Okuma, E., Shiba, H., Kamada, H., Hasegawa, P.M., and Murata, Y. (2013). SIZ1 deficiency causes reduced stomatal aperture and enhanced drought tolerance via controlling salicylic acid-induced accumulation of reactive oxygen species in *Arabidopsis*. Plant J. **73**:91–104.

Murtas, G., Reeves, P.H., Fu, Y.F., Bancroft, I., Dean, C., and Coupland, G. (2003). A nuclear protease required for flowering-time regulation in *Arabidopsis* reduces the abundance of SMALL UBIQUITIN-RELATED MODIFIER conjugates. Plant Cell **15**:2308–2319.

Naseem, M., Kaltdorf, M., and Dandekar, T. (2015). The nexus between growth and defence signalling: auxin and cytokinin modulate plant immune response pathways. J. Exp. Bot. **66**:4885–4896.

Nicholas, K.B., and Nicholas, H.B.J. (1997). GeneDoc: a tool for editing and annotating multiple sequence alignments.

Rasband, W.S. (1997-2009). ImageJ (Bethesda (MD): U. S. National Institutes of Health), Available online at: http://rsb.info.nih.gov/ij/.

Reiter, K., Mukhopadhyay, D., Zhang, H., Boucher, L.E., Kumar, N., Bosch, J., and Matunis, M.J. (2013). Identification of biochemically distinct properties of the small ubiquitin-related modifier (SUMO)

conjugation pathway in plasmodium falciparum. J. Biol. Chem. **288**:27724–27736.

Reiter, K.H., Ramachandran, A., Xia, X., Boucher, L.E., Bosch, J., and Matunis, M.J. (2015). Characterization and structural insights into selective E1-E2 interactions in the human and *Plasmodium falciparum* SUMO conjugation systems. J. Biol. Chem. **291**:3860–3870.

Ribet, D., Hamon, M., Gouin, E., Nahori, M.A., Impens, F., Neyret-Kahn, H., Gevaert, K., Vandekerckhove, J., Dejean, A., and Cossart, P. (2010). Listeria monocytogenes impairs SUMOylation for efficient infection. Nature **464**:1192–1195.

Roden, J., Eardley, L., Hotson, A., Cao, Y., and Mudgett, M.B. (2004). Characterization of the *Xanthomonas* AvrXv4 effector, a SUMO protease translocated into plant cells. Mol. Plant Microbe Interact. **17**:633–643.

Saleh, A., Withers, J., Mohan, R., Marques, J., Gu, Y., Yan, S., Zavaliev, R., Nomoto, M., Tada, Y., and Dong, X. (2015). Posttranslational modifications of the master transcriptional regulator NPR1 enable dynamic but tight control of plant immune responses. Cell Host Microbe **18**:169–182.

Sanchez-Duran, M.A., Dallas, M.B., Ascencio-Ibanez, J.T., Reyes, M.I., Arroyo-Mateos, M., Ruiz-Albert, J., Hanley-Bowdoin, L., and Bejarano, E.R. (2011). Interaction between geminivirus replication protein and the SUMO-conjugating enzyme is required for viral infection. J. Virol. **85**:9789–9800.

Saracco, S.A., Miller, M.J., Kurepa, J., and Vierstra, R.D. (2007). Genetic analysis of SUMOylation in *Arabidopsis*: conjugation of SUMO1 and SUMO2 to nuclear proteins is essential. Plant Physiol. **145**:119–134.

Stulemeijer, I.J., and Joosten, M.H. (2008). Post-translational modification of host proteins in pathogen-triggered defence signalling in plants. Mol. Plant Pathol. **9**:545–560.

Tomanov, K., Hardtke, C., Budhiraja, R., Hermkes, R., Coupland, G., and Bachmair, A. (2013). SUMO conjugating enzyme with active site mutation acts as dominant negative inhibitor of SUMO conjugation in *Arabidopsis*. J. Integr. Plant Biol. **55**:75–82.

van den Burg, H.A., Kini, R.K., Schuurink, R.C., and Takken, F.L. (2010). *Arabidopsis* small ubiquitin-like modifier paralogs have distinct functions in development and defense. Plant Cell **22**: 1998–2016.

Villajuana-Bonequi, M., Elrouby, N., Nordstrom, K., Griebel, T., Bachmair, A., and Coupland, G. (2014). Elevated salicylic acid levels conferred by increased expression of ISOCHORISMATE SYNTHASE 1 contribute to hyperaccumulation of SUMO1 conjugates in the *Arabidopsis* mutant early in short days 4. Plant J. **79**:206–219.

Walden, H., Podgorski, M.S., Huang, D.T., Miller, D.W., Howard, R.J., Minor, D.L., Jr., Holton, J.M., and Schulman, B.A. (2003). The structure of the APPBP1-UBA3-NEDD8-ATP complex reveals the basis for selective ubiquitin-like protein activation by an E1. Mol. Cell **12**:1427–1437.

Wang, J., Hu, W., Cai, S., Lee, B., Song, J., and Chen, Y. (2007). The intrinsic affinity between E2 and the Cys domain of E1 in ubiquitin-like modifications. Mol. Cell **27**:228–237.

Wang, J., Lee, B., Cai, S., Fukui, L., Hu, W., and Chen, Y. (2009). Conformational transition associated with E1-E2 interaction in small ubiquitin-like modifications. J. Biol. Chem. **284**:20340–20348.

Wang, J., Taherbhoy, A.M., Hunt, H.W., Seyedin, S.N., Miller, D.W., Miller, D.J., Huang, D.T., and Schulman, B.A. (2010). Crystal structure of UBA2ufd-Ubc9: insights into E1-E2 Interactions in SUMO Pathways. PLoS One **5**:e15805.

Wang, H.D., Makeen, K., Yan, Y., Cao, Y., Sun, S.B., and Xu, G.H. (2011). OsSIZ1 regulates the vegetative growth and reproductive development in rice. Plant Mol. Biol. Report **29**:411–417.

Xu, P., Yuan, D., Liu, M., Li, C., Liu, Y., Zhang, S., Yao, N., and Yang, C. (2013). AtMMS21, an SMC5/6 complex subunit, is involved in stem cell niche maintenance and DNA damage responses in *Arabidopsis* roots. Plant Physiol. **161**:1755–1768.

Yoo, C.Y., Miura, K., Jin, J.B., Lee, J., Park, H.C., Salt, D.E., Yun, D.J., Bressan, R.A., and Hasegawa, P.M. (2006). SIZ1 SUMO E3 ligase facilitates basal thermotolerance in *Arabidopsis* independent of salicylic acid. Plant Physiol. **142**:1548–1558.

Zinzalla, G. (2013). Understanding and Exploiting Protein? Protein Interactions as Drug Targets (London: Future Science Ltd), pp. 2–4.